ChemComm

Accepted Manuscript

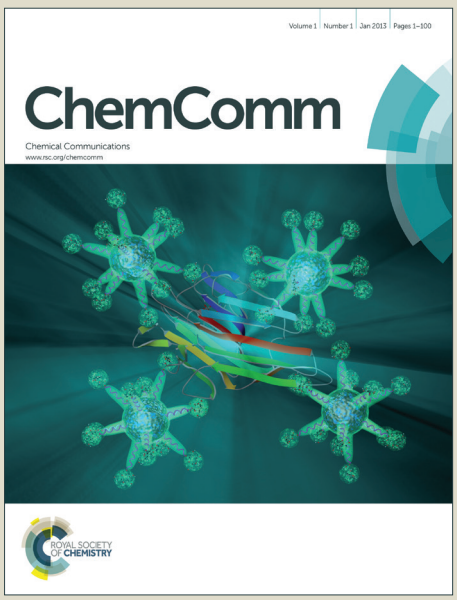

ROYAL SOCIETY OF CHEMISTRY

www.rsc.org/chemcomm

ChemComm

RSCPublishing

COMMUNICATION

Triblock Peptide-Linker-Lipid Molecular Design Improves Potency of Peptide Ligands Targeting Family B G Protein-Coupled Receptors

Cite this: DOI: 10.1039/x0xx00000x

Received 00th January 2012,
Accepted 00th January 2012

DOI: 10.1039/x0xx00000x

www.rsc.org/

Yuting Liu,[†a] Yingying Cai,[†a] Wei Liu,[a] Xiao-Han Li,[a] Elizabeth Rhoades[bc] and Elsa C. Y. Yan[*a]

Two peptide-linker-lipid constructs were designed and prepared which target parathyroid hormone 1 receptor, a family B G protein-coupled receptor. Both show increased agonist activity in a cell-based assay. The lipid moiety enables the formation of micelle-like nanostructures, which is shown to hinder proteolytic digestion and is expected to reduce renal clearance.

G protein-coupled receptors (GPCRs) constitute the largest class of integral membrane proteins in the human genome.[1] They mediate intracellular signaling upon external stimuli and are thus involved in a broad spectrum of biological processes, such as cellular metabolism and neuronal signaling.[1] While all sharing a similar 7-helical transmembrane architecture, GPCRs are often divided into five main sub-families (A-E) based on structural and functional differences.[2] GPCRs have been heavily studied and exploited as drug targets, with most focus on family A GPCRs, the largest subgroup among the five.[3] Recently, family B GPCRs, despite comprising only 15 members, have attracted increasing attentions, especially as drug targets for metabolic diseases, exemplified by osteoporosis and diabetes.[4] Receptors in this family possess an extracellular N-terminal ligand binding domain with a size of ~15 kD. The native ligands of all family B GPCRs are peptides,[5] making the discovery of small-molecule drug candidates extremely challenging. Currently, all drugs on market targeting family B GPCRs are peptides or peptide-derivatives.[5] However, peptide-based drugs generally suffer from facile metabolic degradations by peptidases and via renal clearance,[6] which significantly shortens the half-life of these drugs, rendering large doses necessary while leading to high costs.

To tackle the issue of short lifetime, peptide drug candidates have been chemically modified. For instance, peptoids[7] and β-peptides[8] have been utilized extensively to substitute vulnerable natural peptides as therapeutics. For example, an α/β-peptide analogue of glucagon-like peptide-1 (GLP-1) displayed prolonged action *in vivo*.[9] Conjugation of peptides to transport enhancers represents another well-sought approach to increase the metabolic stabilities of peptide drugs. An illustrative example is PEGASYS,[10] a conjugate of interferon-α with a PEG chain, which is used clinically to treat chronic hepatitis C. Additionally, aside from improving the biostabilities, attachment of lipophilic units, such as membrane-bound peptides[11] and lipid moieties,[12] to bioactive peptides can also evidently enhance membrane association. A few examples include the successful use of the recombinant membrane-tethered ligand technology to optimize bioactivity of peptide ligands targeting incretin receptors,[13] palmitoylation of a short peptide with sequences derived from an intracellular loop of GPCRs to modulate the G protein coupling process,[14] and conjugation of a fatty acid to the GLP-1(7-37) peptide to increase *in vivo* lifetime.[15] We, hereby, conceived an alternative design using a triblock peptide-linker-lipid construct (Fig. 1a) instead of the commonly used diblock analogues to target the extracellular domain of family B GPCRs. This approach led to significant improvements in both bioactivity and biostability.

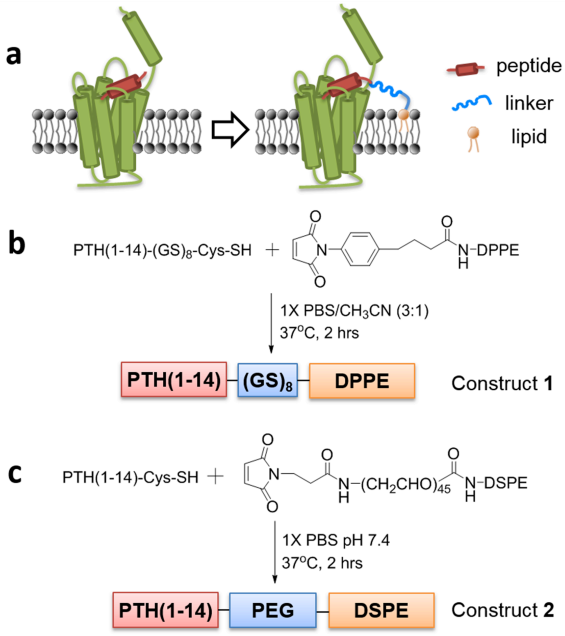

Fig. 1 Design and synthesis of the triblock peptide-linker-lipid construct targeting PTH1R. (a) Schematic view of the triblock constructs (*red*, parental peptide; *blue*, linker; *orange*, lipid). Synthetic schemes for (b) PTH(1-14)-$(GS)_8$-lipid and (c) PTH(1-14)-PEG-lipid.

In our triblock peptide-linker-lipid design, the therapeutic peptide is chemically connected, via a linker group, to a lipid molecule (Fig. 1a). The peptide region serves as the pharmacophore which target the receptor to modulate physiological responses. The linker provides flexibility to allow for optimal peptide-receptor recognition. The lipid component is incorporated to improve the potency based on the following hypotheses: (1) the lipid molecules will partition into lipid membrane to increase the effective concentration of the peptide pharmacophore at membrane surfaces whereby the targeted receptors are located;[16] and (2) the lipid molecule will enable formations of micelle-like nanostructures to alleviate renal clearance and protease degradation.[17]

As a proof of concept, we selected a family B GPCR, parathyroid hormone 1 receptor (PTH1R), as our target. This receptor, highly expressed in the bone osteoblasts and kidney tubule epithelial cells, regulates calcium and phosphate homeostasis and organ developments.[18] This receptor can be activated by two endogenous ligands, parathyroid hormone 1 (PTH) and parathyroid hormone-related protein (PTHrP), leading to G_s coupling and subsequently the activation of the cAMP-dependent pathway.[18] The native PTH ligand contains 84 amino acids while its truncated version, PTH(1-34), has been introduced to the market as a drug to treat osteoporosis.[5]

In this study, we designed and synthesized two constructs targeting PTH1R. Both constructs share the same messenger peptide, PTH(1-14), a weak PTH1R agonist with half maximal effective concentration (EC_{50}) around 100 μM in activating the cAMP pathway.[19] Such weak activity allows for easier determination of improvement in potency. This peptide is appended to two different linkers whereby the linker for construct **1** consists of eight repeating of glycine-serine (GS) units (Fig. 1b) and the linker for construct **2** is polyethylene glycol (PEG) possessing forty-five monomeric units (Fig. 1c). 1,2-dipalmitoyl-sn-glycero-3-phosphoethanolamine (DPPE) is used as the lipid anchor for construct **1** while 1,2-dioctadecanoyl-sn-glycero-3-phosphoethanolamine (DSPE) is selected for construct **2**. Phosphoethanolamine (PE) is chosen because of its ubiquity in cell membranes.[20]

We synthesized the peptide-linker-lipid constructs via a thiol-maleimide coupling reaction (Fig. 1b and 1c).[21] The peptides were modified with a C-terminal cysteine to provide a reactive thiol group while maleimide functionalities were introduced to the lipids. The $(GS)_8$ linker group was incorporated into the peptide sequence through solid-supported synthesis (Fig. 1b); the $(PEG)_{45}$ linker was merged onto the lipid molecule (Fig. 1c) obtained commercially from Avanti Polar Lipid. The thiol-maleimide coupling reaction was monitored using LC-MS; the final products were purified using reverse-phase HPLC (Fig. S1 and S3) and subsequently, lyophilized to the powder form. The molecular weight and purity of the products were confirmed by LC-MS (Fig. S2 and S4).

The bioactivity of the constructs was then determined in a cell-based cAMP enzyme-linked immunosorbent assay (ELISA) using HEK293S cells stably transfected with the PTH1R gene.[22] PTH(1-14)-Cys, without a linker and a lipid anchor, induces intracellular cAMP accumulation with an EC_{50} of 74.6 ± 8.4 μM (Fig. 2), in agreement with the reported value for PTH(1-14).[19] The PTH(1-14)-$(GS)_8$-Cys peptide displays an EC_{50} of 82.1 ± 10.2 μM, indicating the addition of the $(GS)_8$ linker alone has minimal influence on potency. Conversely, lipidated constructs exhibit remarkable improvements over cellular activities: the PTH(1-14)-PEG-lipid construct gives an EC_{50} of 8.0 ± 0.6 μM , representing a 10-fold increase while the PTH(1-14)-$(GS)_8$-lipid construct give an EC_{50} of 0.72 ± 0.17 μM, showing an improvement of 100 folds,.

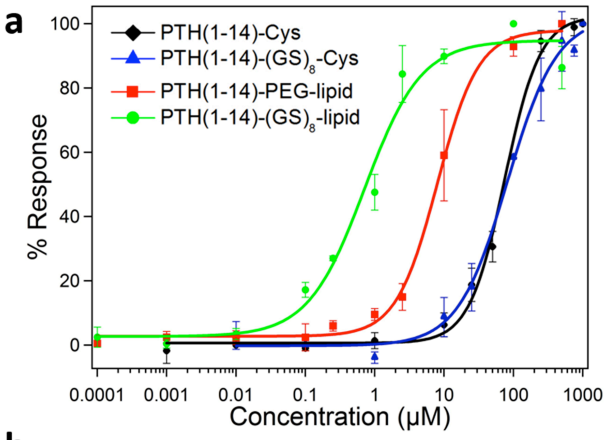

b

(Lipo)peptides	EC_{50} (μM)
PTH(1-14)-Cys	74.64 ± 8.36
PTH(1-14)-$(GS)_8$-Cys	82.07 ± 10.20
PTH(1-14)-PEG-lipid	8.00 ± 0.62
PTH(1-14)-$(GS)_8$-lipid	0.715 ± 0.169

Fig. 2 Designed triblock peptide-linker-lipid constructs enhance PTH1R signaling in HEK293S cells overexpressing PTH1R. (a) Ligand-induced cAMP production measured by ELISA. (b) Calculated EC_{50}s of the triblock peptide-linker-lipid constructs and their parental peptides. Both peptide-linker-lipid constructs displayed higher agonist activity compared to their parental peptides. Error shows average ± SD (n=3).

The improved bioactivity may be attributed to the lipid component in the triblock construct that anchors the peptide into membranes to increase effective concentrations at cell surfaces. To test this hypothesis, we harnessed fluorescence correlation spectroscopy (FCS) to examine the insertion of the PTH(1-14)-$(GS)_8$-lipid construct into lipid membranes, using nanodiscs as the model membrane. These are disk-shaped nanoparticles containing a lipid bilayer stabilized by two membrane scaffold proteins (inset, Fig. 3). The sixth serine residues in the linker region of both PTH(1-14)-$(GS)_8$-Cys and PTH(1-14)-$(GS)_8$-lipid were replaced with a lysine that was covalently connected to a fluorophore, tetramethylrhodamine (TAMRA) (inset, Fig. 3). FCS measurements were made in the absence and presence of nanodiscs. Both peptides exhibit similar diffusion times ($\tau_D \sim 0.25$ ms) in the absence of the nanodiscs, consistent with the rapid diffusion rates expected of small peptides (Fig. 3). Upon the addition of 160 nM nanodiscs, the diffusion time of PTH(1-14)-$(GS)_8$-lipid increases significantly ($\tau_D \sim 0.97$ ms) while that of PTH(1-14)-$(GS)_8$-Cys remains unchanged (Fig. 3). The lipid conjugates showed similar diffusion times compared to labeled nanodiscs,[23] indicating the insertion of PTH(1-14)-$(GS)_8$-lipid into the nanodisc bilayer has taken place. These results suggest that the lipid component can direct the triblock construct to the membrane and therefore, increase the local concentration, possibly leading to higher potencies.

Owing to the presence of the lipid motifs, the triblock constructs were hypothesized to form nanostructures in aqueous environments. We attempted to verify this by probing into the self-assembly processes of the two triblock constructs. First, we used size exclusion chromatography (SEC) and transmission electron microscopy (TEM) to estimate the sizes of the nanostructures formed by the constructs. The gel filtration profile for the $(PEG)_{45}$-

linker construct, taken at 2.9 mM, shows a major peak at 9.2 mL (Fig. 4a), corresponding to a Stokes diameter of 15.8 nm. The $(GS)_8$-linker construct (0.8 mM), on the other hand, shows a major peak at 11.8 mL (Fig. 4a) in the profile, corresponding to a Stokes diameter of 11.7 nm. The TEM images (Fig. 4b) indicate that the average particle sizes for the $(PEG)_{45}$-linker and $(GS)_8$-linker constructs are 13.6 nm and 8 nm, respectively. The $(PEG)_{45}$-linker construct forms slightly larger nanoparticles in aqueous solution than the $(GS)_8$-linker construct. This may be explained by comparing their linker lengths: $(PEG)_{45}$-linker is about ~20 nm[24] while the $(GS)_8$-linker is ~5 nm long. Second, we determined the critical micelle concentration (CMC), the minimal concentration for formation of micelle nanostructures, using the surface tension method.[25] The constructs were added into PBS subphase (1.8 mM KH_2PO_4, 10 mM Na_2HPO_4, 2.7 mM KCl and 137 mM NaCl, PH 7.4) in a Langmuir trough and the surface tension was recorded as a function of concentration of the two triblock constructs (Fig. 4c). From these plots, the CMCs were determined to be 0.199 μM for the $(GS)_8$-linker construct and 0.154 μM for the $(PEG)_{45}$-linker construct. The $(PEG)_{45}$-linker construct possesses a slightly lower CMC value compared to the $(GS)_8$-linker construct, suggesting its higher tendency to form micelle nanostructures. This may be rationalized in terms of carbon chain lengths where the DSPE (18:0) lipid in the $(PEG)_{45}$-linker construct has longer chains than the DPPE (16:0) lipid in the $(GS)_8$-linker construct.

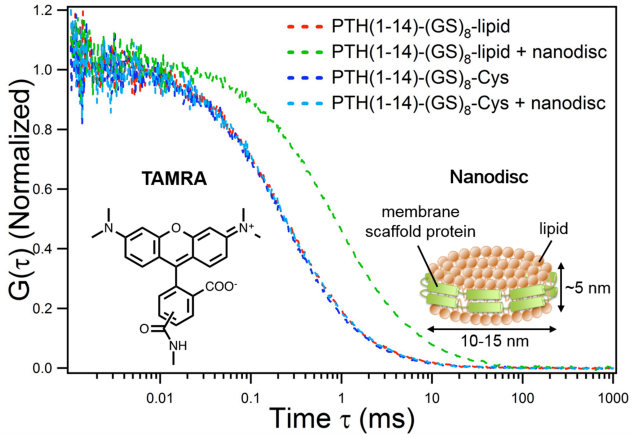

Fig. 3 Insertion of the triblock peptide-linker-lipid constructs into nanodiscs. Normalized autocorrelation curves of 50 nM TAMRA-labeled peptide with (red and green curves) and without (blue and cyan curves) lipid conjugation. Upon addition of 160 nM nanodisc, the autocorrelation curve shifts to the right only for the peptide with lipid conjugation, PTH(1-14)-$(GS)_8$-lipid (green curve), but not the peptide without lipid conjugation, PTH(1-14)-$(GS)_8$-Cys (cyan curve), The right-shifted autocorrelation curve indicates that PTH(1-14)-$(GS)_8$-lipid has a longer diffusion time in the presence of nanodiscs, suggesting of insertion of PTH(1-14)-$(GS)_8$-lipid into nanodiscs. Inset shows the structures of TAMRA (left) and a nanodisc (right), in which two copies of the membrane scaffold protein wraps around the edge of a lipid bilayer.

The constructs' tendencies to form nanoparticles were postulated to impede proteolytic degradations: we examined this by comparing the protease digestion rates of PTH(1-14)-$(GS)_8$-Cys and PTH(1-14)-$(GS)_8$-lipid. Experimentally, both constructs were incubated at concentrations above their CMCs in the presence of trypsin at ambient temperature for 10 mins after which the digested mixtures were immediately separated using reverse phase HPLC (See ESI). PTH(1-14)-$(GS)_8$-Cys is completely degraded (Fig. 5), while over 75% of PTH(1-14)-$(GS)_8$-lipid remained undigested. PTH(1-14)-$(GS)_8$-Cys' proteolytic fraction elutes at 29% acetonitrile. It has a molecular mass of 1455 Da, corresponding to the amino acid sequence of SVSEIQLMHNLGK (Fig. 5a). Likewise, when PTH(1-14)-$(GS)_8$-lipid is cleaved, two digested fractions were obtained which elutes at 29% (not shown) and 81% acetonitrile respectively. They showed molecular masses of 1455 and 1049 Da, corresponding to the amino acid sequence of SVSEIQLMHNLGK and the cysteine conjugated lipid tail (Cys-lipid) (Fig. 5b). These results suggest that lipid conjugation can effectively reduce proteolytic degradation, which is likely due to the steric hindrance provided by the micelle-like nanostructures.

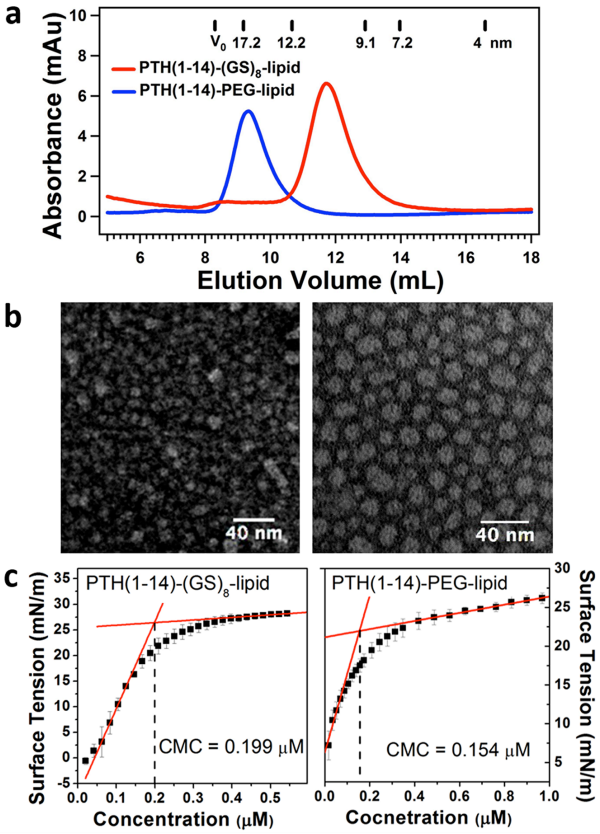

Fig. 4 Lipopeptide constructs form nanostructures in solution. (a) Gel filtration curves of the lipopeptides. The PTH(1-14)-$(GS)_8$-lipid (red curve) nanostructure has a Stokes diameter of 11.7 nm, while that for the PTH(1-14)-$(PEG)_{45}$-lipid (blue curve) nanostructure is 15.8 nm. (b) TEM images of the lipopeptides. The average sizes are 8 nm and 13.6 nm for the PTH(1-14)-$(GS)_8$-lipid and PTH(1-14)-PEG-lipid nanostructures, respectively. (c) Surface tension measurement. The CMCs for PTH(1-14)-$(GS)_8$-lipid and PTH(1-14)-PEG-lipid are 0.199 μM and 0.154 μM, respectively.

All together, the experimental results above support our proposal that the triblock peptide-linker-lipid design can enhance both bioactivity and biostability. Higher activity results when lipid tails insert into membranes, leading to increased local concentrations. The stability, on the other hand, stems from self-assemblies of nanostructures that evidently slow down proteolytic degradation.

Notably, as shown in the cell-based ELISA, the $(GS)_8$-linker construct is approximately 10 times more potent compared to the $(PEG)_{45}$-linker construct (Fig. 2). This difference likely arises from their distinct chemical nature and particularly, the lengths of the two linkers. The $(PEG)_{45}$-linker construct (~20 nm) is longer than the $(GS)_8$-linker (~5 nm) - it is possible that a longer hydrophilic linker renders the construct's partition in aqueous phase more thermodynamically favourable, reducing its localization on the cell surface. In addition, given the fact that the N-terminal ligand binding domain of PTH1R has the size of a few nanometers, the $(GS)_8$-linker

(~5 nm long) may facilitate the peptide's binding to the N-terminal ligand binding domain better while the $(PEG)_{45}$-linker (~20 nm) may be too long and too flexible for optimal binding. Indeed, studies are underway to optimize the linker lengths in the triblock peptide-linker-lipid constructs for higher potencies. The dramatically different potency enhancements brought about by $(GS)_8$-linker and $(PEG)_{45}$-linker evidently underscore the value of the triblock design, where the linker group can be used as a chemical tool to modulate the partitioning of the constructs into biomembrane while optimizing peptide-receptor interactions for higher potencies.

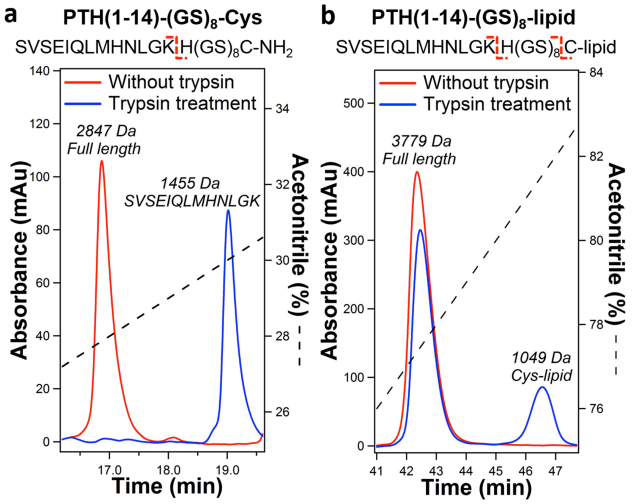

Fig. 5 Proteolytic degradation of (a) PTH(1-14)-$(GS)_8$-Cys and (b) PTH(1-14)-$(GS)_8$-lipid in the presence of trypsin (peptide: trypsin = 100:1) (blue lines). After 10 min enzyme treatment, peptides were separated using a reverse phase HPLC. Superimposed to these chromatograms are the profiles of peptides without trypsin treatment (red lines). PTH(1-14)-$(GS)_8$-Cys was degraded completely, while PTH(1-14)-$(GS)_8$-lipid remained largely intact (75%). Potential cleavage sites are indicated.

The concept of triblock design where a peptide is lipidated via a flexible linker group should be applicable to all transmembrane drug targets whose native ligands are peptides - selectivity can be achieved by tailoring the sequence of the messenger peptides for specific transmembrane targets. Hence, further optimizations of individual peptide, linker, and lipid components in the triblock constructs targeting PTH1R and other family B GPCRs will contribute to a general strategy to improve potencies of peptide-based therapeutics for a wide range of transmembrane drug targets.

Acknowledgement

This work is supported by the Yale Setup fund. E. C. Y. Y. is the recipient of NSF Career Grant (MCB-0955407). The NIH grant (NS079955) is awarded to E. R.

Notes and references

[a] Department of Chemistry, Yale University, New Haven, CT 06520;
[b] Department of Molecular Biophysics and Biochemistry, Yale University, New Haven, CT 06520;
[c] Department of Physics, Yale University, New Haven, CT 06520.
[†] These authors contributed equally to this manuscript.

Electronic Supplementary Information (ESI) available: Experimental procedures and supplementary figures. See DOI: 10.1039/c000000x/

1 M. C. Lagerstrom and H. B. Schioth, *Nat. Rev. Drug Discov.*, 2008, **7**, 339.
2 R. Fredriksson, M. C. Lagerstrom, L. G. Lundin and H. B. Schioth, *Mol. Pharmacol.*, 2003, **63**, 1256.
3 (a) B. K. Shoichet and B. K. Kobilka, *Trends Pharmacol. Sci.*, 2012, **33**, 268; (b) C. Seibert and T. P. Sakmar, *Curr. Pharm. Des.*, 2004, **10**, 2041; (c) X. Y. Ding, X. Zhao and A. Watts, *Biochem. J.*, 2013, **450**, 443; (d) U. Alexiev and D. L. Farrens, *Biochim. Biophys. Acta.*, 2014, **1837**, 694; (e) E. Mathew, A. Bajaj, S. M. Connelly, H. Sargsyan, F. X. Ding, A. G. Hajduczok, F. Naider and M. E. Dumont, *J. Mol. Biol.*, 2011, **409**, 513.
4 D. R. Poyner and D. L. Hay, *Br. J. Pharmacol.*, 2012, **166**, 1.
5 J. K. Archbold, J. U. Flanagan, H. A. Watkins, J. J. Gingell and D. L. Hay, *Trends Pharmacol. Sci.*, 2011, **32**, 591.
6 D. J. Craik, D. P. Fairlie, S. Liras and D. Price, *Chem. Biol. Drug Des.*, 2013, **81**, 136.
7 R. N. Zuckermann and T. Kodadek, *Curr. Opin. Mol. Ther.*, 2009, **11**, 299.
8 E. V. Denton, C. J. Craig, R. L. Pongratz, J. S. Appelbaum, A. E. Doerner, A. Narayanan, G. I. Shulman, G. W. Cline and A. Schepartz, *Org. Lett.*, 2013, **15**, 5318.
9 L. M. Johnson, S. Barrick, M. V. Hager, A. McFedries, E. A. Homan, M. E. Rabaglia, M. P. Keller, A. D. Attie, A. Saghatelian, A. Bisello and S. H. Gellman, *J. Am. Chem. Soc.*, 2014, **136**, 12848.
10 M. W. Fried, M. L. Shiffman, K. R. Reddy, C. Smith, G. Marinos, F. L. Goncales, Jr., D. Haussinger, M. Diago, G. Carosi, D. Dhumeaux, A. Craxi, A. Lin, J. Hoffman and J. Yu, *N. Engl. J. Med.*, 2002, **347**, 975.
11 J. P. Fortin, Y. Zhu, C. Choi, M. Beinborn, M. N. Nitabach and A. S. Kopin, *Proc. Natl. Acad. Sci. U. S. A.*, 2009, **106**, 8049.
12 (a) A. Malina and Y. Shai, *Biochem. J.*, 2005, **390**, 695; (b) C. Aicart-Ramos, R. A. Valero and I. Rodriguez-Crespo, *Biochim. Biophys. Acta.*, 2011, **1808**, 2981; (c) L. Zhang and G. Bulaj, *Curr. Med. Chem.*, 2012, **19**, 1602.
13 J. P. Fortin, D. Chinnapen, M. Beinborn, W. Lencer and A. S. Kopin, *PLoS One*, 2011, **6**, e24693.
14 (a) P. Dimond, K. Carlson, M. Bouvier, C. Gerard, L. Xu, L. Covic, A. Agarwal, O. P. Ernst, J. M. Janz, T. W. Schwartz, T. J. Gardella, G. Milligan, A. Kuliopulos, T. P. Sakmar and S. W. Hunt, 3rd, *Ann. N. Y. Acad. Sci.*, 2011, **1226**, 34; (b) L. Covic, A. L. Gresser, J. Talavera, S. Swift and A. Kuliopulos, *Proc. Natl. Acad. Sci. U. S. A.*, 2002, **99**, 643.
15 D. Russell-Jones, *Mol. Cell Endocrinol.*, 2009, **297**, 137.
16 T. Y. Wang, R. Leventis and J. R. Silvius, *Biochemistry*, 2001, **40**, 13031.
17 M. Avadisian and P. T. Gunning, *Mol. Biosyst.*, 2013, **9**, 2179.
18 M. Mannstadt, H. Juppner and T. J. Gardella, *Am. J. Physiol.*, 1999, **277**, F665.
19 N. Shimizu, J. Guo and T. J. Gardella, *J. Biol. Chem.*, 2001, **276**, 49003.
20 D. R. Voelker, in *Biochemistry of Lipids, Lipoproteins And Membranes*, ed. J. E. Vance, Elsevier, 2008, pp. 441-484.
21 J. Kalia and R. T. Raines, *Curr. Org. Chem.*, 2010, **14**, 138.
22 N. Mitra, Y. Liu, J. Liu, E. Serebryany, V. Mooney, B. T. DeVree, R. K. Sunahara and E. C. Yan, *ACS Chem. Biol.*, 2013, **8**, 617.
23 A. Nath, A. J. Trexler, P. Koo, A. D. Miranker, W. M. Atkins and E. Rhoades, *Method Enzymol.*, 2010, **472**, 89.
24 T. W. Chung, D. Z. Liu, S. Y. Wang and S. S. Wang, *Biomaterials*, 2003, **24**, 4655.
25 A. Patist, S. S. Bhagwat, K. W. Penfield, P. Aikens and D. O. Shah, *J. Surfactants Deterg.*, 2000, **3**, 53.

